# A Mathematical Approach to the Connectivity Between the Cortical Visual Areas of the Macaque Monkey

Bertrand Jouve, Pierre Rosenstiehl and Michel Imbert

Centre de Recherche Cerveau et Cognition – UMR 5549, Faculté de Médecine de Rangueil, 133 route de Narbonne, 31062 Toulouse Cedex and Centre d'Analyse et de Mathématique Sociales, EHESS, 54 Boulevard Raspail, 75270 Paris Cedex 06, France

**The visual cortex of the macaque monkey is divided into many distinct visual information processing areas. In many cases, anatomical and physiological results allow one to determine the presence or the absence of neuronal connections from one area to another. We have approached the topology of this neuronal network within the mathematical framework of graph theory. At first, we studied the unknown part of the network, i.e. the part where anatomical and physiological results are lacking. Relying on a specific topological property of the network established on the known part, we developed an interpolation algorithm for reducing the level of uncertainty concerning the unknown part. From these results, we then constructed a connectional model of the neuronal network for the entire cortical visual system. Subsequently, a topological analysis of this model, with the help of factorial analysis and clustering technics, shows its structural properties and singular vertices. This analysis suggests the existence of two distinct classes of areas, one in the parietal part of the cortex and the other in the temporal part, which are connected to each other via relay areas, especially involving the frontal eye field. These results may help to understand the functional role of particular cortical areas in vision and, more generally, to explore how visual information flows within the visual cortex.**

## 1. Introduction

### *1.1 Graph Theory and Factorial Analysis: A Rigorous Framework*

Visual information processing is performed within many distinct areas of the cerebral cortex of the macaque monkey. These areas are connected in a network of neurons transmitting signals specific to each processed attribute. The network can be symbolized by an oriented graph. Our aim is to reveal topological properties of this graph that may help understand the role of some cortical visual areas in vision and, more generally, how visual information flows within the cerebral cortex. About 32 visual areas have been identified on the basis of anatomical and physiological experiments (Felleman and Van Essen, 1991). In section 1.2 we list the references that have been used to construct the matrix of the network's connections. Roughly a quarter of the network still remains unknown. In this paper we first try to reduce this uncertainty. We describe a specific topological property, called $P$, derived from the known part of the visual network that is then extended to the entire network for making predictions (2.2.3: algorithm). This provides a topological model $G_1$ of the cortical visual system. In section 3 we use two competing methods, factorial analysis and clustering, to analyze the topology of this model. The main idea of these methods is that local computations on a graph can reveal its global structure. The local computation selected here is a measure of local connectivity represented by an Euclidean distance $d$ on the set of vertices of the graph. The influence on the global structure of the graph is revealed by studying the representation, in a multidimensional Euclidean space, of an isometric embedding (see section 3 and appendix 3 for mathematical details) of the graph with respect to the distance $d$. The crossing over from local to global is made using factorial analysis or clustering methods. This study extends to oriented graphs the methods of a previous work (Kuntz, 1992) on non-oriented graphs, which analyzed the connections of aircraft electrical systems.

All the algorithms used in this paper were written in the C language on an i486 running under OS2.

To lighten the paper, all the notations and basic definitions proper to graph theory or factorial analysis have been put in appendices (appendices 1 and 3). The reader should refer to these for mathematical details.

### *1.2 Experimental Data and Anatomical Connection Network*

We shall suppose the visual cortex of the macaque monkey to be divided into 32 different areas. Four types of criteria are generally used to identify them: connectivity criteria, as revealed by retrograde and/or anterograde tracers; structural criteria, revealed by histological staining techniques (Nissl, myelin, cytochrome oxidase, neurofilament protein) (Hof and Morrison, 1995; Tootell and Taylor, 1995); topographic criteria, derived from receptive field mapping; and physiological criteria based on response selectivity.

The various visual areas are principally connected by the axons of neurons running through the white matter. While the pattern of connections has been extensively studied by many laboratories, it is at present still incompletely understood. Our work is based on a matrix of connections between visual areas, derived from the work of Felleman and Van Essen (1991). This matrix is a square binary matrix. The value at the intersection of row $i$ and column $j$ indicates the existence (1) or the absence (0) of a projection from area $i$ to area $j$. Although Felleman and Van Essen introduced large + symbol and minor + symbol in their connectivity table so as not to give the same credence to every connection, working with binary matrix prevents us from such distinctions. So, we make no difference between a large + symbol and a minor + symbol, and both of these connections are given a value equal to 1. In the same table, a value of (0) is given to dots corresponding to non-connections (connections tested and found absent). We neglect any asymmetry in the chance of false (0) versus false (1), because these are difficult to estimate and probably vary considerably even if false (0) are much less likely than false (1) if one considers anatomical methodology. Then, following Young (1992), we assign connections from or to PIT, CIT and STP respectively from or to PITd and PITv, CITd and CITv, and STPp and STPa. We do not include areas MIP and MDP in the matrix because of lack of connection data.

Following results from other authors, we include some

**Table 1**
Adjacency matrix of $G_1$, model of the connection network of the visual system

| $G_1$ to from | V1 | V2 | V3 | VP | V3A | MT | MST d | MST l | PO | PIP | LIP | VIP | V4 | VOT | V4 t | FST | DP | 7a | FEF | PIT d | PIT v | CIT d | CIT v | AIT d | AIT v | STP p | STP a | TF | TH | 46 | No. of successors | No. of predecessors |
|---|---|---|---|---|---|---|---|---|---|---|---|---|---|---|---|---|---|---|---|---|---|---|---|---|---|---|---|---|---|---|---|---|
| V1 | 1 | 1 | 1 | 0 | 1 | 1 | 0 | **0** | 1 | 1 | 0 | 0 | 1 | 0 | 0 | 0 | 0 | 0 | 0 | 0 | 0 | 0 | 0 | 0 | 0 | 0 | 0 | 0 | 0 | 0 | 7 | 8 |
| V2 | 1 | 1 | 1 | 1 | 1 | 1 | 1 | 1 | 1 | 1 | 0 | 1 | 1 | 1 | 1 | 1 | 0 | 0 | **1** | 0 | 0 | 0 | 0 | 0 | 0 | 0 | 0 | 0 | 0 | 0 | 15 | 16 |
| V3 | 1 | 1 | 1 | **1** | 1 | 1 | 1 | 0 | 1 | 1 | 1 | 1 | 1 | **1** | 1 | 1 | **1*** | 0 | **1** | 0 | **0** | 0 | 0 | 0 | 0 | 0 | 0 | 1 | 0 | 0 | 17 | 16 |
| VP | 0 | 1 | 1 | 1 | 1 | 1 | 1 | 0 | 1 | 1 | **1** | 1 | 1 | 1 | 0 | 1 | 1* | 0 | 1 | 0 | 0 | 0 | 0 | 0 | 0 | 0 | 0 | 1 | 0 | 0 | 15 | 14 |
| V3A | 1 | 1 | 1 | 1 | 1 | 1 | 1 | 1 | 1 | **1** | 1 | 1 | 1 | 1 | 1 | 1 | 1 | 0 | 1 | 0 | 0 | 0 | 0 | 0 | 0 | 0 | 0 | 0 | 0 | 0 | 17 | 17 |
| MT | 1 | 1 | 1 | 1 | 1 | 1 | 1 | 1 | 1 | 1 | 1 | 1 | 1 | **1** | 1 | 1 | 0 | 0 | 1 | 0 | 0 | 0 | 0 | 0 | 0 | 0 | 0 | 0 | 0 | 1* | 17 | 16 |
| MST d | 0 | 1 | 1 | 1 | 1 | 1 | 1 | **1** | 1 | 1 | 1 | 1 | 0 | 0 | 1 | 1 | 1 | 1 | 1 | 1* | 0 | 0 | 0 | 0 | 0 | 1 | 1* | 1 | 1* | 1* | 21 | 17 |
| MST l | 0 | 1 | 0 | 0 | 1 | 1 | **1** | 1 | 1 | 0 | 1 | 1 | 0 | 0 | 1 | 1 | 1 | 1 | 1 | 0 | 0 | 0 | 0 | 0 | 0 | 1 | 1* | 0 | 1* | 1* | 16 | 14 |
| PO | 1 | **1** | 1 | 1 | 1 | 1 | 1 | 1 | 1 | 1 | 1 | 1 | 0 | 0 | 1 | 0 | 1 | 1 | 1 | 0 | 0 | 0 | 0 | 0 | 0 | 0 | 0 | 0 | 0 | 0 | 15 | 16 |
| PIP | 1 | **1** | 1 | 1 | 1 | 1 | 1 | 1* | 1 | 1 | 1 | 1 | 1 | 1 | 1 | 1* | 1 | 1* | 1 | 0 | 0 | 0 | 0 | 0 | 0 | 0 | 0 | 1* | 0 | 1* | 20 | 15 |
| LIP | 0 | **1*** | 1 | 1 | 1 | 1 | 1 | 1 | 1 | 1 | 1 | 1 | 1 | 1 | 1 | 1 | 1 | 1 | 1 | 0 | 1 | 0 | 0 | 0 | 0 | 0 | 0 | 1 | 0 | 1* | 20 | 18 |
| VIP | 0 | **1** | 1 | 1 | 1 | 1 | 1 | 1 | 1 | 1 | 1 | 1 | 1* | 1 | 1 | 1 | 1 | 1 | 1 | 0 | 0 | 0 | 0 | 0 | 0 | 0 | 0 | 1* | 0 | 1* | 19 | 16 |
| V4 | 1 | 1 | 1 | 1 | 1 | 1 | 0 | 0 | 0 | 1 | 1 | 0 | 1 | 1 | 1 | 1 | 1 | 0 | **1** | 1 | 1 | 1 | 1 | 0 | 1 | 0 | 0 | 1 | 1 | 1* | 21 | 21 |
| VOT | 0 | 1 | **1** | 1 | 1 | 1 | 0 | 0 | 1* | 1 | 1 | 1 | 1 | 1 | 1 | 1 | 1* | 0 | 1 | 1 | 1 | 1 | 1 | 0 | 1 | 0 | 0 | 1 | 0 | 1 | 21 | 21 |
| V4 t | 1* | **1** | 1 | 0 | 1 | 1 | 1 | 1 | 1 | 1 | 1 | 1 | 1 | 1 | 1 | 1 | 1 | 1 | 1 | 1 | 1 | 1 | 1 | 0 | 1 | 1 | 1 | 1 | 1 | 1 | 27 | 27 |
| FST | 0 | **1** | 1 | 1 | 1 | 1 | 1 | 1 | 0 | 0 | 1 | 1 | 1 | 1 | 1 | 1 | 0 | 1 | 1 | 1 | 1 | 0 | 0 | 0 | 0 | 1 | 1* | 1 | 1 | 0 | 20 | 23 |
| DP | 0 | 0 | 0 | 0 | 1 | 0 | 1 | 1 | 1 | 1 | 1 | **1** | 1 | **0** | **1** | 1* | 1 | 1 | **1** | 0 | 0 | 0 | 0 | 0 | 0 | 0 | 0 | 0 | 0 | 1 | 13 | 25 |
| 7a | 0 | 0 | 0 | 0 | 0 | 0 | 1 | **1** | 1 | 0 | 1 | **1** | 0 | **0** | **1** | 1 | 1 | 1 | 1 | 0 | 0 | 0 | 0 | 1 | **0** | 1 | 1 | 1 | 1 | 1 | 15 | 16 |
| FEF | 0 | **1** | 1 | 1 | 1 | 1 | 1 | 1 | 1 | 1 | 1 | 1 | 1 | 1 | 1 | 1 | 1 | 1 | 1 | 1 | 1 | 1 | 1 | 1 | 1 | 1 | 1 | 1 | 1 | 1 | 28 | 28 |
| PIT d | 0 | 0 | 0 | 0 | 0 | 0 | **0** | 0 | 0 | 0 | 0 | 0 | 1 | 1 | 1 | 1 | 1* | 0 | 1 | 1 | 1 | 1 | 1 | 1 | 1 | 1 | 1 | 1 | 1 | 1 | 16 | 16 |
| PIT v | 0 | 0 | **0** | 0 | 0 | 0 | 0 | 0 | 0 | 0 | 1 | 0 | 1 | 1 | 1 | 1 | 1* | 0 | 1 | 1 | 1 | 1 | 1 | 1 | 1 | 0 | 0 | 1 | 0 | 1 | 14 | 14 |
| CIT d | 0 | 0 | 0 | 0 | 0 | 0 | 0 | 0 | 0 | 0 | 0 | 0 | 1 | **1** | **1** | 1* | **1*** | 0 | 1 | **1** | 1 | 1 | **1** | 1 | 1 | **1** | **1** | **1** | **1** | 1 | 16 | 14 |
| CIT v | 0 | 0 | 0 | 0 | 0 | 0 | 0 | 0 | 0 | 0 | 0 | 0 | 1 | 1 | **1** | 1* | **1*** | 0 | 1 | **1** | 1 | **1** | 1 | 1 | 1 | **1** | **1** | **1** | **1** | 1 | 16 | 14 |
| AIT d | 0 | 0 | 0 | 0 | 0 | 0 | 0 | 0 | 0 | 0 | 0 | 0 | 0 | **1*** | **1*** | 0 | **1*** | 1 | 1 | **1** | 1 | **1** | 1 | 1 | **1** | **1*** | **1** | **1** | **1** | 1 | 15 | 11 |
| AIT v | 0 | 0 | 0 | 0 | 0 | 0 | 0 | 0 | 0 | 0 | 0 | 0 | 1 | 1 | **1** | 0 | **1*** | **0** | **1** | **1** | 1 | **1** | 1 | **1** | 1 | **1** | 0 | 1 | 1 | **1** | 14 | 13 |
| STP p | 0 | 0 | 0 | 0 | 0 | 0 | 1 | 1 | 0 | 0 | 0 | 0 | 0 | 0 | **1** | 1 | **1*** | 1 | 1 | **1** | 0 | 1 | 1 | 0 | **1** | 1 | 1 | 1 | 1 | 1 | 15 | 15 |
| STP a | 0 | 0 | 0 | 0 | 0 | 0 | **0** | 0 | 0 | 0 | 0 | 0 | 0 | 0 | 1 | 0 | 1* | 1 | 1 | 1 | 0 | 1 | 1 | 1 | 0 | 1 | 1 | 1 | 1 | 1 | 12 | 14 |
| TF | 0 | 0 | 1 | 1 | 0 | 0 | 1 | **0** | 0 | 0 | 1 | 0 | 1 | 1 | 1 | 1 | 1* | 1 | 1 | 1 | 1 | 1 | 1 | 1 | 1 | 1 | 1 | 1 | 1 | 1 | 21 | 22 |
| TH | 0 | 0 | 0 | 0 | 0 | 0 | 0 | 0 | 0 | 0 | 0 | 0 | 1 | 1* | **1** | **1** | **1*** | 1 | **1** | **1** | 1* | 1 | 1 | 1 | 1 | 1 | 1 | **1** | 1 | 1 | 17 | 16 |
| 46 | 0 | 0 | 0 | 0 | 0 | **0** | 0 | 0 | 0 | **0** | **0** | **0** | **0** | **1** | **1** | 0 | 1 | 1 | 1 | **1** | **1** | 1 | 1 | 1 | **1** | 1 | 1 | 1 | 1 | 1 | 15 | 22 |

Normal type corresponds to known pairs (connections revealed as existing or absent by previous published anatomical or physiological experiments), whereas the 223 entries in bold type correspond to predicted values of unknown pairs. Asterisks indicate non-reciprocal connections.

additional connections to those listed by Felleman and Van Essen. These connections are from MT to 46 (Barbas, 1988), from MT to PO (Colby *et al.*, 1988), from CITd, CITv and 7a to FST (Boussaoud *et al.*, 1990), from V4, CITv, AITv, TF, TH, LIP and FEF to VOT, from FST, PITd and FEF to PITv, from VOT to FST, CITv, AITv, TF and LIP, from PITv to FST, PITd, TF, LIP, FEF and 46 (Distler, 1993).

Also, we posit as non-existent some connections considered as unknown by Felleman and Van Essen: from STPp, STPa, MSTd and MSTl to VOT and PITv, from VOT and PITv to STPp, STPa, TH and MSTd, from VOT to MSTl (Distler, 1993).

Finally, recent results (Distler, 1993) go against the data revealed by Felleman and Van Essen and assign non-connections between VOT and TEO (including here areas VOT and PITv). Therefore, we consider the connections between these areas as unknown.

The matrix of connections we arrive at is a 30 × 30 matrix with 324 known connections, 323 known non-connections and 223 unknown pairs. We call unknown pair an oriented pair $(i,j)$ of areas $i$ and $j$ for which we do not know if there exists or not a direct projection from $i$ to $j$.

## 2. A Model of the Visual System

Throughout this presentation $G_\infty = \{V_\infty, E_\infty\}$ will represent the graph of the visual system of the macaque monkey, where $V_\infty$ is the set of the 30 visual cortex areas and $E_\infty$ is the set of the connections between visual cortical areas. The set $E_\infty$ is not fully known but it includes the 324 connections of the matrix of connections revealed by physiological and anatomical experiments. In order to allow a topological study of the graph $G_\infty$, we looked for a method reducing the uncertainty about the unknown pairs. In the following, we denote $G_0 = \{V_\infty, E_0, N_0, U\}$ the graph where $E_0$ is the set of the 324 known connections of the visual system, $N_0$ the set of the 323 known non-connections, and $U$ the set of the 223 unknown pairs. In other words, $G_0$ represents what we know about $G_\infty$ (Table 1). Thus, $G_\infty$ is a supergraph of the graph $G_0$ (see Appendix 1 for definitions). From the graph $G_0$, we will construct a graph $G_1$, supergraph of $G_0$ and without unknown pairs, approaching $G_\infty$ in the way that the number of pairs that are different between $G_1$ and $G_\infty$ has good reasons to be low. Notice that all the graphs in this paper are oriented graphs.

### *2.1 An Index of Connectivity*

**Definition 1** *Given two vertices i and j of a graph, we call indirect connection from i to j a walk of length 2 from i to j, i.e. a sequence of vertices i, k, j where (i,k) and (k,j) are two arcs of the graph.*

In the following we shall be strongly concerned by a positive correlation between the existence of the connection $(i,j)$ and the existence of indirect connections from $i$ to $j$.

**Definition 2** *Given a graph G and its adjacency matrix A(G) = $(a_{ij})$, for each ordered pair of vertices (i,j), with $i \neq j$, we define the index of connectivity c by:*

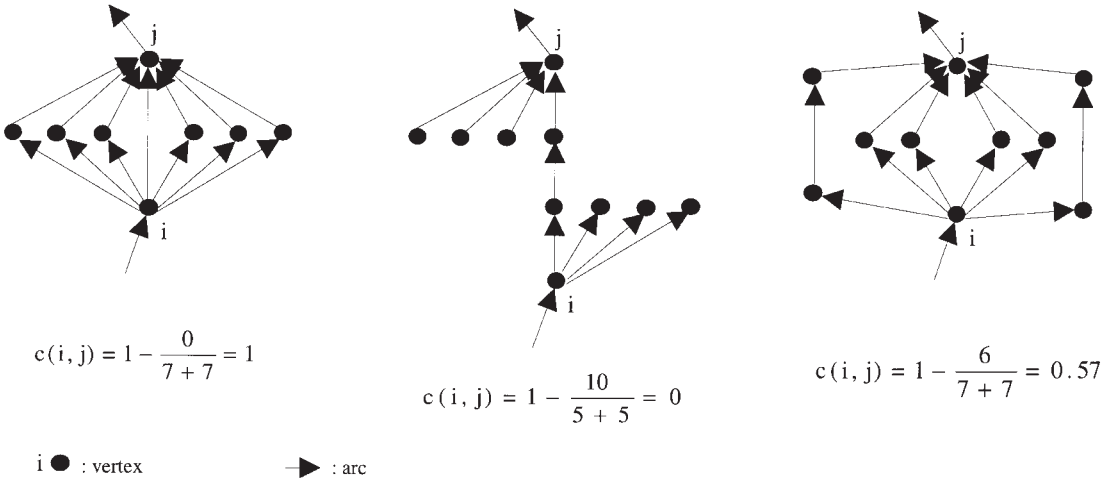


**Figure 1.** Example of some calculations of the index of connectivity *c* for the arc (*i*,*j*).

$$c(i,j) = 1 - \frac{\sum_{k=1}^{n} \left| a_{ik} - a_{kj} \right|}{\sum_{k=1}^{n} \left( a_{ik} + a_{kj} \right)}$$

The index $c(i,j)$ is high if and only if there are many successors of $i$ among the predecessors of $j$ and many predecessors of $j$ among the successors of $i$. More precisely, it is equal to twice the number of indirect connections divided by the total number of arcs incident from the vertex $i$ plus the total number of arcs incident to the vertex $j$. It gets its values from the interval [0;1] and quantifies what we call in the following: *a proportion of indirect connections from the vertex i to the vertex j*. In Figure 1, we calculate $c$ on some examples. It is clear that generally $c(i,j) \neq c(j,i)$.

### *A Distribution Property of the Connections Between the Cortical Visual Areas*

*Analysis of the Known Pairs*

Among the known pairs, we notice that a connection $(i,j)$ is nearly always accompanied by many indirect connections (cf. definition 1) from $i$ to $j$, and a non-connection by very few indirect connections. So we have analyzed the distribution of the values of the index $c$ (cf. definition 2) over the set of the known pairs of the graph $G_0$, looking for the threshold values $\varepsilon$ of $c$ such that a high percentage of connections has a value of $c$ above $\varepsilon$ and a high percentage of non-connections has a value of $c$ below $\varepsilon$. For that sake, we define two functions $\alpha$ and $\beta$ of $c$ that, in statistical terms, are cumulative increasing frequencies of the index $c$ on the set of the connections and non-connections.

**Definition 3** *Given a graph G and a parameter* $\tau \in [0;1]$*, we denote* $\alpha(\tau)$ *the percentage of connections (i,j) of G such that* $c(i,j) < \tau$*, and* $\beta(\tau)$ *the percentage of non-connections (i,j) of G such that* $c(i,j) \leq \tau$.

We are interested in a value of $\tau$ for which $|\beta(\tau) - \alpha(\tau)|$ is maximum. Thus, we also define the threshold $\varepsilon$ of a graph as:

**Definition 4** *Given a graph G, we define the connectivity threshold* $\varepsilon$ *of G to be the largest value of* $\tau$ *for which* $|\beta(\tau) - \alpha(\tau)|$ *is maximum.*

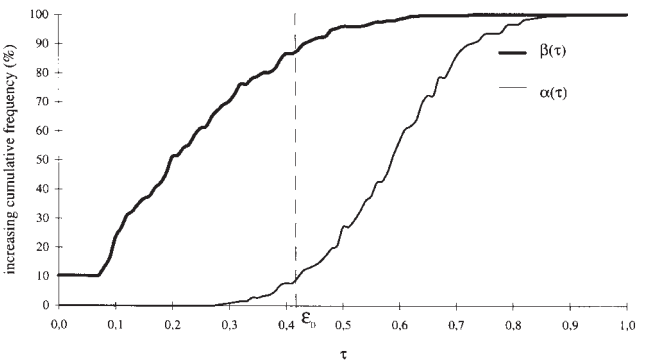


**Figure 2.** Distribution of the values of the index of connectivity *c* between the areas of the visual system for the known pairs. The bold curve is the graph of the $\alpha$ function, and the other curve represents the $\beta$ function. These functions are cumulative increasing frequencies of the index of connectivity *c* on the set of the 324 known connections and the set of the 323 known non-connections (see definition 3 for more details). The threshold 0.41 of the index of connectivity *c* is the highest value of *c* for which the distance between the two curves is maximum. It separates the connections from the non-connections with an error of 10%.

For the graph $G_0$, $\varepsilon_0 = 0.41$ is such a threshold with $\alpha(\varepsilon_0) = 7\%$ and $\beta(\varepsilon_0) = 87\%$ (Fig. 2). In other words, 93% of the connections are between areas whose value $c(i,j)$ is above 0.41, and 87% of the non-connections are between areas whose value $c(i,j)$ is below 0.41 [notice that we gave the value (0) in $A(G_0)$ to each unknown pair]. Most of the connections link vertices between which there is a high proportion of indirect connections, whereas most of the non-connections correspond to pairs with a low proportion of indirect connections. This property, which we shall denote $P$, dictates how areas connect to each other. The following definition is a modeling of it.

**Definition 5** *Given a graph G = {V,E,N,U} and its connectivity threshold* $\varepsilon$*, we say that:*

- *a known pair (i,j) has the property P if and only if* $c(i,j) \geq \varepsilon$ *for a connection (i,j) and* $c(i,j) \leq \varepsilon$ *for a non-connection (i,j).*
- *the graph G has the property P if >90% of its known pairs (i,j) have the property P.*

This definition means that a graph has the property $P$ if the index of connectivity $c$ (cf. definition 2) separates the

**Table 2**

Mean values of the 223 computed pairs over 50 graphs *G* provided by the interpolation algorithm from $G_0$

| to / from | V1 | V2 | V3 | VP | V3A | MT | MST d | MST l | PO | PIP | LIP | VIP | V4 | VOT | V4 t | FST | DP | 7a | FEF | PIT d | PIT v | CIT d | CIT v | AIT d | AIT v | STP p | STP a | TF | TH | 46 |
|---|---|---|---|---|---|---|---|---|---|---|---|---|---|---|---|---|---|---|---|---|---|---|---|---|---|---|---|---|---|---|
| V1 | | | | | | | | 6* | | | | | | | | | | | 88 | | | | | | | | | | | |
| V2 | | | | | | | | | | | | | | | | | | | | | | | | | | | | | | |
| V3 | | | | 100* | | | | | | | | | | 84 | | | 63 | | 90 | | 0* | | | | | | | | | |
| VP | | | | | | | | | | | 100* | | | | | | 61 | | 94* | | | | | | | | | | | |
| V3A | | | | | | | | | | 100* | 100* | 100* | | 71 | 94* | | | | 90 | | | | | | | | | | | |
| MT | | | | | | | | | | | | | | 73 | | | | | | | | | | | | | | | | |
| MST d | | | | | | | | 100* | | 76 | | | | | | | | | | | | | | | | | 69 | 86 | 51 | 94* |
| MST l | | | | | | | 100* | | | | 90 | | | | 96* | | 90 | 100* | | | | | | | | | 76 | 22 | 55 | 88 |
| PO | | 98* | 94* | 73 | 100* | | | | | 92* | | | | 49 | 69* | | | | 67 | | | | | | | | | | | 33 |
| PIP | | 100* | | | 100* | | 100* | 100* | | | 100* | 100* | | 82 | 96* | 100* | | | 98* | | | | | | | | | 76 | 0* | 69 |
| LIP | | 100* | | | | | | | | 92* | | | | | 100* | | | | | | | | | | | 20 | 10 | | | |
| VIP | | 98* | | 94* | 98* | | | | | 86 | | | 90 | 78 | 96* | | 96* | | | | | | | | | 37 | 43 | 80 | 43 | 88 |
| V4 | | | | | | | | | | | | | | | | | | | 100* | | | | | | | | | | | |
| VOT | | | 86 | | 71 | 71 | | | 55 | 67 | | 65 | | | 90 | | 82 | 31 | 98* | | | 51 | | 43 | | | | | | 92* |
| V4 t | | 94* | | | 100* | | 100* | | | 71 | 100* | 92* | | 82 | | | 96* | 92* | 92* | 67 | 63 | 57 | 61 | 49 | 55 | 69 | 69 | 78 | 63 | 86 |
| FST | | 98* | | 96* | | | | | | | | | | | | | | | | | | | | | | | 61 | | 57 | |
| DP | | | | | | | | | | | | 100* | | 41 | 84 | | | | 78 | | | | | | | | | | | |
| 7a | | | | | | | | 98* | | 0* | | 67 | | 39 | 90 | | | | | | | | | | 6* | | | | | |
| FEF | | 73 | 80 | 69 | 88 | 78 | | | | 57 | | | 96* | | 98* | | | | | 98* | | | | | 80 | | 84 | 100* | 84 | |
| PIT d | | | | | | | 0* | | | | | | | | 82 | | 78 | | | | | 98* | | | | 82 | 71 | 199* | 84 | |
| PIT v | | | 2* | | | | | | | | | | | 100* | 80 | | 78 | | | | | 92* | | 94* | | | | | | |
| CIT d | | | | | | | | | | | | | | 98* | 80 | | 80 | | | 100* | | | 100* | | | 84 | 80 | 100* | 90 | |
| CIT v | | | | | | | | | | | | | | | 82 | | 82 | | | 100* | | 98* | | | | 84 | 78 | 100* | 92* | |
| AIT d | | | | | | | | | | | | | | 67 | 67 | | 82 | | | 92* | | 98* | | | 96* | 96* | 86 | 98* | 94* | |
| AIT v | | | | | | | | | | | | | | | 69 | | 84 | 14 | 86 | 100* | | 96* | | 98* | | 59 | | | | 98* |
| STP p | | | | | | | | | | | | | | | 88 | | 86 | | | 96* | | | | | 69 | | | | | |
| STP a | | | | | | | 4* | 6* | | | | | | | 53 | 33 | 63 | | 65 | 84 | | 90 | 92* | | | | | | | |
| TF | | | | | | | | 2* | | | 96* | | | | 90 | | 96* | | 100* | 100* | | 96* | | | | | | | 98* | |
| TH | | | | | | | | | | | | | | | 86 | 100* | 88 | | 100* | 100* | | | | | | | | 100* | | |
| 46 | | | | | | 0* | | 8* | 0* | 0* | 8* | 0* | 47 | 67 | 82 | | | | | 90 | 96* | | | | 94* | | | | | |

These percentages may be understood as an index of reliability of the computed pairs. The 106 asterisked entries correspond to the most probable interpolations (values below 10% or over 90%).

connections from the non-connections with an error of <10%; the error being the percentage of known pairs that do not have the property *P*.

*2.2.2 Conjecture*

The graph $G_0$ has the property *P* (cf. section 2.2.1) and two strong arguments encourage us to extend this property *P* to the whole graph $G_\infty$. Firstly, the sample set of the known pairs of the graph $G_\infty$ is large enough (75% of the graph ). Secondly, the iteration of the property P is a Hebb rule (Hebb, 1949), which figures prominently in models of visual system development (Madison *et al.*, 1991). Hence, we make the following conjecture:

**Conjecture** *$G_\infty$ has the property P.*

As the graph $G_0$ has 223 unknown pairs and 324 connections, the percentage of connections of $G_\infty$ may vary from 37 to 62%. Among all the supergraphs of $G_0$, very few satisfy the property *P*; we checked this fact by a Monte-Carlo method using 50 random supergraphs of $G_0$ with a density varying from 37 to 62%: none of them appears to have the property *P*. This property seems to be a good control property for the search of $G_1$, the graph approaching $G_\infty$.

*2.2.3 Reduction of Uncertainty for the Unknown Pairs: Selection of a Model*

*Presentation of the Interpolation Algorithm.* Given a graph *G* that is not entirely known, which has the property *P*, and given its threshold ε, the algorithm of the interpolation of the unknowns uses the following rule:

*i* is adjacent to *j* if and only if $c(i,j)$ is below the threshold ε

It signifies that to decide if an unknown pair is a connection or a non-connection, we just have to look at the proportion of indirect connections quantified by the index of connectivity *c*. Roughly, if the proportion is high, it is a connection, and conversely, if the proportion is low, it is a non-connection. Let $G_0$ be a graph with *N* unknown pairs. Firstly we construct a graph $\tilde{G}_0$ which is a supergraph of $G_0$ where the *N* unknown pairs are randomly given the value (0) or (1) for the initialization of the computing. Then, we construct a series of graphs ($\tilde{G}_k$) in the following way:

- Let us suppose that the graph $\tilde{G}_k$ is constructed, and denote by $\tilde{\varepsilon}_k$ its threshold. We point to the unknown pair of $\tilde{G}_k$ which value $|c(i,j) - \tilde{\varepsilon}_k|$ is the largest, this pair loses its status as an unknown pair and is assigned a value (0) or (1) according to its position with regard to the threshold. In that way, we reach the new graph $\tilde{G}_{k+1}$, and in the event of *p* unknown pairs simultaneously maximize the value $|c(i,j) - \tilde{\varepsilon}_k|$ we directly reach graph $\tilde{G}_{k+p}$.
- The process stops when there are no more unknown pairs, thus defining a graph $\tilde{G}_N$.

We make $M = 100$ iterations. The number of (1) randomly given to the unknowns varies from 0 to *N* throughout the *M* iterations. These *M* tests therefore provide *M* graphs $\tilde{G}_N$. We choose the test, and the corresponding graph $\tilde{G} = \tilde{G}_N$, with

$\tilde{G} = \tilde{G}_N$

$\tilde{\varepsilon}_k$

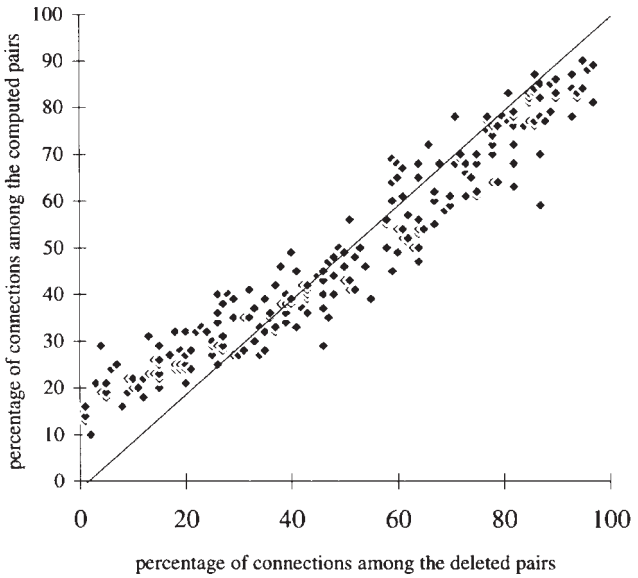


**Figure 3.** To test our interpolation algorithm, a mean of 220 pairs have been deleted in 231 different graphs with 30 vertices which have the property *P*. We have used our algorithm to try to recover these deleted pairs. In order to verify that our algorithm does not overestimate the connections, we have plotted the percentage of connections among the computed pairs as a function of the percentage of connections among the deleted pairs.

$\tilde{G}$ $\left|\beta(\tilde{\varepsilon}_0)-\alpha(\tilde{\varepsilon}_0)\right|+\left|\beta(\tilde{\varepsilon}_N)-\alpha(\tilde{\varepsilon}_N)\right|$ maximum. $\tilde{G}$ is a supergraph of the graph $G_0$ with no unknown pairs. By construction, the graph $\tilde{G}$ has the property *P*.

*Convergence of the Algorithm and Selection of the Model.* We test the convergence of the algorithm by computing 50 supergraphs $\tilde{G}$ of the graph $G_0$, and comparing them arc by arc. The graphs $\tilde{G}$ differ, on average, in 48 edges on 870 possible (5.5%), with a standard error of 13. If the values of the unknown pairs had been chosen at random, two graphs $\tilde{G}$ would differ, on average, in 112 connections (13%) (cf. Appendix 2). So, if our conjecture is valid, the number of possible topological models for the visual system is divided by more than two. Moreover, 106 unknown pairs (Table 2) take the same value (0) or (1) in >90% of the graphs $\tilde{G}$. This suggests that their probability of belonging to $G_\infty$ is very high. Thus, they are good candidates for anatomical or physiological testing. Finally, we construct the graph $G_1$ as the mean of the 50 computed supergraphs $\tilde{G}$ in the sense that a pair of $G_1$ is an arc if and only if it is an arc in at least half of the graphs $\tilde{G}$. We consider that $G_1$ is an approximation of $G_\infty$. $G_1$ has a density of 59% (515 connections and 355 non-connections); it contains the 647 known pairs $(i,j)$ of $G_0$ plus 223 computed pairs. The threshold $\varepsilon_1$ of $G_1$ is equal to 0.60, $\alpha(\varepsilon_1)$ to 5%, and $\beta(\varepsilon_1)$ to 92%.

*Quality of the Algorithm.* For testing the quality of interpolation of the algorithm, we verify its capacity for recovering supergraphs of $G_0$ with no unknown pairs, with property *P*, from which we deleted at random, on average, 220 pairs. We computed the algorithm on such 231 graphs, and among the deleted pairs the proportion of connections varies uniformly from 1 to 97%. The algorithm restores, on average, 84% of the deleted pairs. The 16% of erroneous pairs are partly explained by the fact that the threshold ε separates the connections from the non-connections with an error of ~10%.

Because the graph $G_1$ has more connections than non-connections, we have verified that the algorithm does not overestimate the connections. For the 231 previous graphs, we have analyzed the percentage of connections among the computed pairs as a function of the percentage of connections among the deleted pairs (Fig. 3). The relation between these two percentages is statistically significant ($r^2$ = 0.93, $P$ = 0.001) and the results reveal a low overestimation when the percentage of deleted connections is below 46%, and, in contrast, a low underestimation otherwise.

In short, if we consider that the graph of the visual system has the property *P*, we have constructed an approximation $G_1$ of it. This model has a predictive value on the unknown pairs of $G_0$. Nearly half of these predictions seems to be very probable.

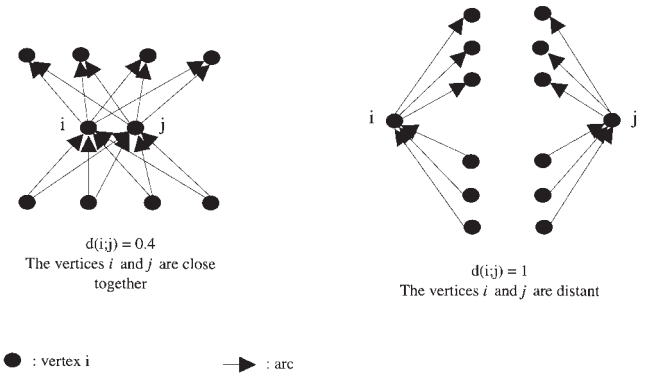


**Figure 4.** Comparison of model DV and area 5 phasic activity during a control task (*a*) and a priming task (*b*), where the target is shown before the 'go' stimulus is given. The times of the target presentation and the 'go' stimulus are shown as a vertical dashed line. This simulation used the same parameters as that of Figure 3. Rasters reprinted from Crammond and Kalaska (1989).

## 3. Topological Analysis of the Model $G_1$

We use two competing methods for studying the topology of the graph $G_1$: factorial analysis and vertex clustering. Both use a representation of the graph in a multidimensionnal space, called an 'embedding' of the graph. In an embedding, the vertices of the graph are not arbitrarily positioned into the space, but positioned so that any two of them, named *i* and *j*, are at a given distance $d(i;j)$. The given distance $d$ is Euclidean and the dimension of the space is at most equal to the number of vertices of the graph minus one. In this way, the local distance $d$ acts on the global form of the cloud of points. Then, depending on the choice of the distance, some particular topological subsets of the graph may be revealed. In our case, we are interested in subgraphs like dense subgraphs, subgraphs with a very low density, or subgraphs without circuits, which may be interpreted in terms of functionality within the visual system. To that end, and guided by a previous study of Kuntz (1992), we have chosen a distance $d$ between the vertices of the graph $G_1$ such that two vertices are close together if and only if they have many common predecessors and few different ones, and many common successors and few different ones (cf. Appendix 3 for mathematical details) (Fig. 4). This distance $d$ reflects the difference in the local connectivity of two vertices. It gives good results with both the following methods of topological analysis.

### *3.1 Factorial Representation of $G_1$*

We realize an embedding of $G_1$ with respect to $d$, previously defined and detailed in Appendix 3, in the space $\mathbb{R}^{29}$. This representation is denoted by $I_d(G_1)$. Note that this distance $d$ is

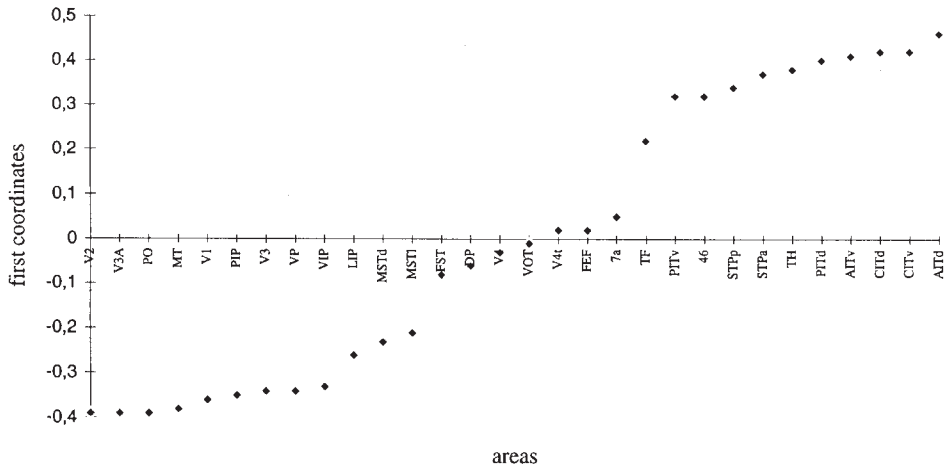


**Figure 5.** Coordinates of the vertices of $I_d(G_1)$ (cortical visual areas) on the first factorial axis arranged in increasing order.

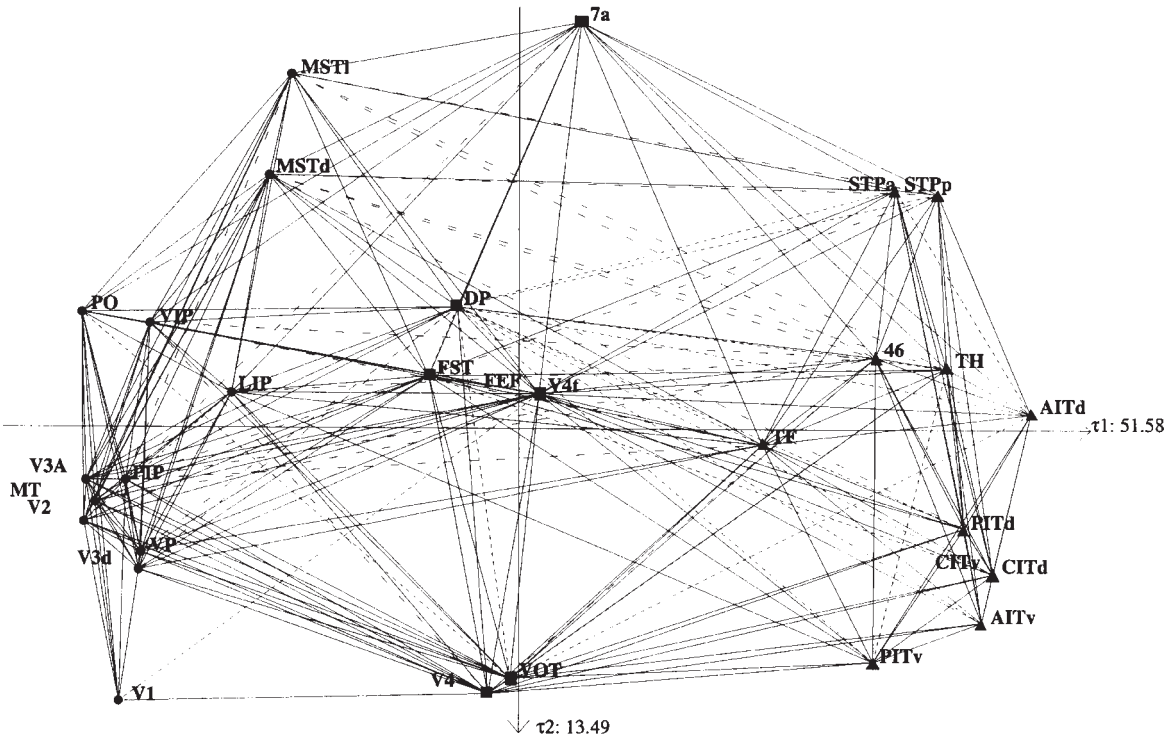


**Figure 6.** Projection of the *d*-representation $I_d(G_1)$ of our model of the visual system onto the plan of the two first factorial axes. The vertices of the dorsal and ventral classes are respectively represented by dots and triangles. 'Relay' areas are represented by squares. Continuous lines show reciprocal connections, lines with long dotted are connections from left to right, and lines with short dotted are connections from right to left.

not supposed to quantify some neurobiological strength of the connection between two cortical areas. The high dimensionality of the space containing $I_d(G)$ does not allow us to have a general idea of the global structure of the graph. Factorial analysis allows us to find and study the axes, called factorial axes, around which the cloud [vertices of $I_d(G_1)$] is organized (see Appendix 3 for details). Generally, the projection of the cloud into the space generated by the first axes allows a large part of the inertia (also called variance in probabilistic terms) to be kept and gives a good idea of the global structure of the graph. In our case, the factorial analysis of $I_d(G_1)$ provides a satisfactory representation in $\mathbb{R}^3$, the space generated by the three first factorial axes. The inertia of the projection of $I_d(G_1)$ onto this space is of 72%.

### *3.1.1 The Three Classes of $G_1$*

The factorial analysis of $G_1$ reveals a first factor which is very important compared with the others, since it represents $\tau_1 = 52\%$ of the total inertia of the cloud. Even if the interpretation of the different projections of $I_d(G_1)$ generally requires knowledge of the biological significance of the different factors, such a first important factor often reflects a structure of the cloud of points in different clusters (Bastin *et al.*, 1980). The first axis separates three classes of areas whose coordinates on this axis are respectively in the intervals [–0.39;–0.21], [–.08;–0.05] and [0.22;0.46] (Fig. 5). The first class, which we call here the dorsal class, contains the areas V1, V2, V3d, VP, V3A, MT, PO, PIP, LIP, VIP, MSTd and MSTl, the second class the areas V4, VOT, FEF,

**Table 3**
Quality of the representation $I_d(G_1)$ in the first factorial plan

| Areas | $COR_1$ | $COR_2$ | $COR_3$ | $COR_1 + COR_2$ | $CTR_1$ | $CTR_2$ | $CTR_3$ |
|---|---|---|---|---|---|---|---|
| CIT d | 82 | 8 | 1 | **90** | 6 | 2 | 1 |
| CIT v | 82 | 8 | 1 | **90** | 6 | 2 | 1 |
| PIT d | 82 | 4 | 0 | **86** | 5 | 1 | 0 |
| V3A | 84 | 1 | 0 | **85** | 5 | 0 | 0 |
| AIT v | 70 | 13 | 1 | **83** | 6 | 4 | 1 |
| MT | 77 | 2 | 0 | **79** | 5 | 0 | 0 |
| TH | 76 | 2 | 2 | **78** | 5 | 0 | 1 |
| V3 | 67 | 10 | 0 | **77** | 4 | 2 | 0 |
| V2 | 73 | 3 | 2 | **76** | 5 | 1 | 1 |
| VIP | 70 | 6 | 3 | **76** | 4 | 1 | 1 |
| PIP | 73 | 1 | 0 | **74** | 4 | 0 | 0 |
| PO | 67 | 5 | 2 | **72** | 5 | 2 | 1 |
| AIT d | 72 | 0 | 2 | **72** | 7 | 0 | 1 |
| STP p | 51 | 21 | 3 | **72** | 4 | 6 | 2 |
| STP a | 54 | 18 | 9 | **72** | 5 | 6 | 6 |
| MST d | 34 | 35 | 0 | **69** | 2 | 7 | 0 |
| MST l | 20 | 49 | 3 | **69** | 1 | 13 | 2 |
| 7a | 1 | 67 | 1 | **68** | 0 | 18 | 1 |
| PITv | 46 | 21 | 2 | **67** | 3 | 6 | 1 |
| VP | 55 | 6 | 1 | **61** | 4 | 2 | 1 |
| 46 | 58 | 3 | 0 | **61** | 3 | 1 | 0 |
| LIP | 50 | 1 | 14 | **51** | 2 | 0 | 5 |
| V4 | 1 | 43 | 9 | **44** | 0 | 7 | 3 |
| VOT | 0 | 44 | 17 | **44** | 0 | 7 | 5 |
| V1 | 29 | 14 | 46 | **43** | 4 | 8 | 51 |
| TF | 40 | 0 | 16 | **40** | 2 | 0 | 5 |
| DP | 2 | 8 | 3 | **10** | 0 | 2 | 1 |
| FST | 5 | 2 | 18 | **7** | 0 | 0 | 5 |
| FEF | 0 | 2 | 28 | **2** | 0 | 0 | 4 |
| V4 t | 0 | 1 | 10 | **1** | 0 | 0 | 2 |

All values are percentages.

$COR_i(j)$ is the contribution of the $i$th factor in the representation of the vertex $j$. $CTR_i(j)$ gives the importance of the vertex $j$ for the $i$th factor.

V4t, FST, DP and 7a, and the third class, which we call here ventral class, the areas PITd, PITv, CITd, CITv, AITd, AITv, STPa, STPp, TF, TH and 46.

*3.1.2 Quality of the Representation on the First Factorial Plan*
The quality of the projection of a cloud of points onto its $i$th factorial axis can be analyzed by two parameters: $COR_i$ and $CTR_i$. $COR_i(j)$ is the contributions of the $i$th factor in the representation of the vertex $j$ and $CTR_i(j)$ gives the importance of the vertex $j$ for the $i$th factor.

Among all the factors superior to one, the contribution $\tau_2$ of the second factor to the total inertia of the cloud of points $I_d(G_1)$ is much more important than the others. In the same way, the high value of $COR_1 + COR_2$ for 26 vertices of the graph $G_1$ (Table 3) shows that most of vertices are well represented in the plan of the two first factorial axes (first factorial plan). The distribution of $CTR_1$ and $CTR_2$ over the vertices of the graph is well balanced. The inertia of these axes also results from all the vertices of the graph and not only from some of them. This confirms the importance of these two factors for the whole graph.

In the first factorial plan, the second class is clearly divided into three groups of areas: V4 and VOT, then FST, FEF, V4t and DP, and finally 7a. Because the relative contributions $COR_1$ and $COR_2$ of the four areas FST, FEF, V4t and DP are very low, the justification of this grouping is to be found in the larger dimensionality of the embedding space. In this way, we have analyzed the projection of these vertices on the third axis. As half of the inertia of the third axis results from the area V1 (Table 3), we have removed this vertex from the graph $G_1$ before analyzing the projection on this axis. This projection supports the grouping of three of these areas: FEF, FST and V4t (Fig. 7).

Note that these areas are very close to the center of gravity of the cloud (Fig. 8). Their position near the center of the first factorial plan is thus justified. On the other hand, even if the membership of the second class for the area DP is not questioned, moving it closer to the three previous areas, as revealed by the first factorial plan, would not be justified. Indeed, this area moves off following the fifth axis [$CTR_5$(DP) = 50% and $COR_5$(DP) = 59%].

Note also that the vertex V1 is the farthest vertex from the center of gravity of the cloud (Fig. 8) and moves off following the third axis [$CTR_3$(V1) = 51% and $COR_3$(V1) = 46%] even if it is not badly represented by its projection onto the first factorial plan.

### *3.2 An Efficient Method for Clustering*

In a general way, a problem of network's partitioning may be defined as the search for a partition of the set of vertices such that the intra-class and inter-class edges verify some specific properties. De Fraysseix and others have described a general framework to efficiently solve a class of partitioning problems relative to electrical networks (de Fraysseix *et al.*, 1992): 'First, a distance is selected on the vertices of the graph, which reflects the properties to be satisfied by the classes of the partition. Second, the graph is partitioned with an iterative method which uses the notion of center of gravity to minimize the intra-class inertia' $\Im(P_k)$ defined by:

**Definition 6** *Let $P_k = (C_1, C_2, ..., C_k)$ be a partition of the set of vertices V in k classes, and $g_i$ the center of gravity of the class $C_i$. We denote $\Im(P_k)$ the intra-class inertia associated to the partition $P_k$:*

$$\Im(P_k) = \frac{1}{n}\sum_{i=1}^{k}\sum_{v_j \in C_i} d^2(v_j, g_i)$$

We used their methodology with the distance $d$ we have previously defined (cf. Appendix 3). Although this method was originally conceived for non-oriented graphs, we here extend it to oriented graphs by separating the successors from the predecessors in the calculus of the distance. The optimal configurations (which minimize this inertia) are made up of dense subgraphs, or subgraphs with a very low density, or subgraphs without circuits, such that any of two classes are linked by reciprocal connections, or by unidirectional connections (i.e. connections which all have the same direction), or are not linked. Notice that this process takes into account the $n - 1$ dimensions of the embedding space, i.e. all the variability of the embedding graph. We use this clustering method to cluster the graph $G_1$ in three classes. It confirms exactly the previous clustering of the visual areas provides by the factorial analysis.

### *Relay Areas*

The three classes of areas generated by both methods of topological analysis define three subgraphs with a high density (respectively 88, 86, 93%). There are very few connections between the dorsal and the ventral classes (only 10% of the total possible arcs linking the two classes), and nearly half of them are unidirectional (13 out of 27), all from the dorsal class to the ventral one (Table 4). On the contrary, 71% of the possible connections between these two classes and the second class are existent and 94% are reciprocal. Therefore, nearly every path between the dorsal and the ventral classes goes through areas of

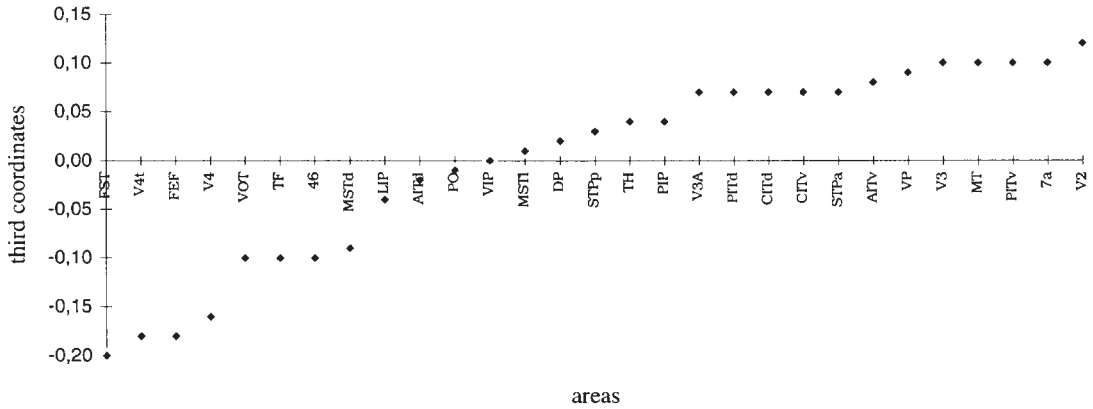


**Figure 7.** Coordinates of the vertices of $I_d(G_1 - \{V1\})$ (cortical visual areas except V1) on the third factorial axis arranged in increasing order.

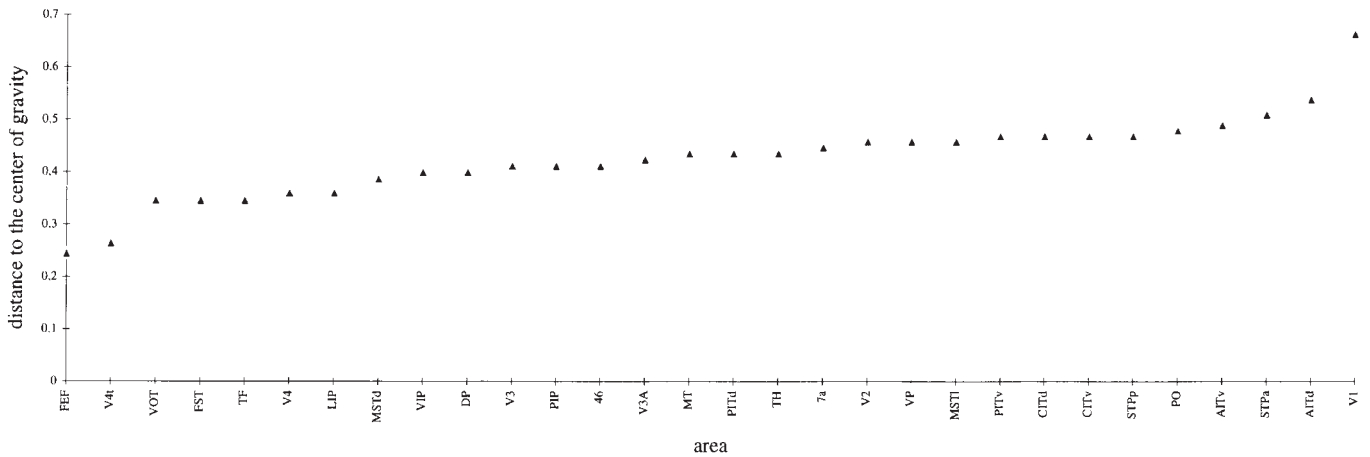


**Figure 8.** Distance $d$ to the center of gravity of the cloud $I_d(G_1)$.

the second class. So, the visual system could be schematized by a graph made up of two dense subgraphs (corresponding to the dorsal and the ventral classes) bound by a set of seven vertices. We chose to call areas of this second class 'relay areas'.

## 4. Discussion

### *4.1 The need to Estimate Missing Data*

We used deterministic graphs, in which the matrix of the connections is binary. There is thus no possible quantification of the unknowns. It is therefore necessary to establish a process of decision that allows one to attribute a value of (0), or of (1), to all unknown values in the connection matrix. This process could be arbitrary. In this case, comparing the results obtained and seeking out structural constants rules over all interpretations. On the other hand, the process can also be guided by various hypotheses regarding the network. In our study, we seek information contained in the known part of the network that could be extended to its whole. The assigning of a value to the unknowns then becomes a process of interpolation. This is what we have done in our work using the derived property P. We used the specific topology appearing on the part of the graph resulting from already published neuroanatomical experiments. The results can then be interpreted directly by simply taking into account the topological hypotheses that have been made. This attempt to estimate missing data is obviously not a shortcut to actually doing the experimental neuroanatomical work. Because we have made a conjecture and because the rate of error of our interpolation seems to be around 16%, our aim is not to 'second guess' neuroanatomy but only to try to reduce the error on the missing data in order to allow better specific models which capture as much of the underlying structural properties of the visual system as possible. However, our predictions might be used to direct future anatomical studies so as to correct our model and to confirm or invalidate our general results concerning the functional organization of the visual system.

**Table 4**
Inter-class and intra-class (on the diagonal) edges for the three classes defined by factorial analysis and clustering

| Class | 1 | 2 | 3 |
|---|---|---|---|
| 1 | 116 | | |
| 2 | 123 | 36 | |
| 3 | 27 | 111 | 102 |

### *4.2 About the Choice of a Distance on the Graph of the Visual System*

The analysis of the geometrical representation of a graph depends on the choice of the distance fitted on it. We have chosen this distance $d$ that takes into account the local

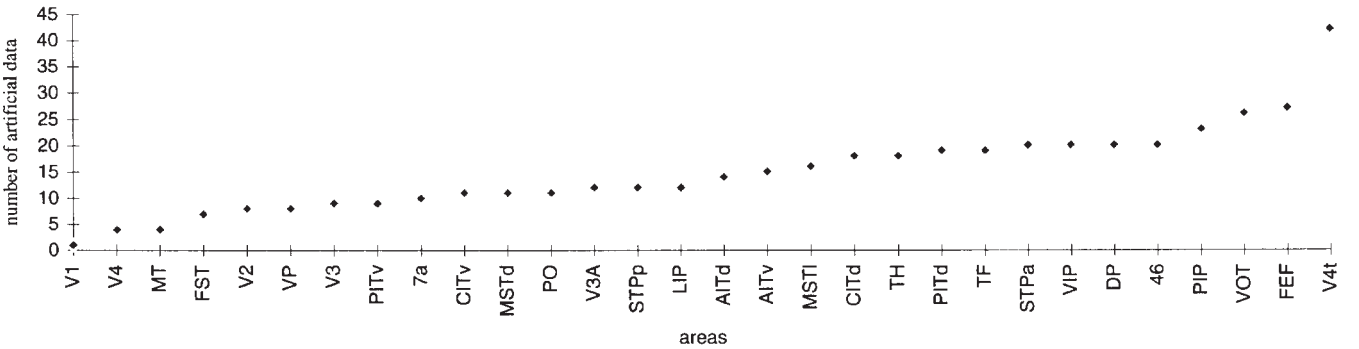


**Figure 9.** Number of artificial data for each visual area in the connectivity matrix, arranged in increasing order. Relay areas could be areas with many artificial data or areas with few artificial data.

connectivity into the graph but different choices would have supplied other interpretations. For instance, the choice of a distance which just takes into account the successors or the predecessors would have allowed some conclusions about processing without loops (examples of such a distance are $d^+$ or $d^-$ defined in Appendix 3). It is possible that the same graph may have two identical geometrical representations with two different distances. In such a case, we may look for the graph's topological properties which explain that result. For instance, if $e(i,j)$ is the shortest path between two vertices $i$ and $j$, it is easy to show that the topological structure of the graph $G_1$ we revealed implies that the distributions of the distances $e(i,j)$ and $d^+(i,j)$ are roughly the same. This applies to some similar representations in the Young *et al.* (1995) paper.

### *4.3 About the Relay Areas*

#### *4.3.1 Some Control Tests*

Among the 223 computed pairs of $G_1$ we have seen that 106 of them have a high probability of being true if $G_\infty$ has the property $P$. We have computed a clustering of two new graphs constructed from $G_1$ by setting the 117 other computed pairs at (0) or at (1). We find again the same structure with two dense classes bound by some 'relay' areas. These areas are VOT, V4, 7a, FEF and FST. This test supports the special status of 'relay areas' given to these five areas.

Moreover, we applied our two methods of factorial analysis and clustering to the two 'control' cases of Young *et al.* (1995): the first is obtained by setting all the unknowns at (0) and the second by setting them at (1). The representations we arrived by projection onto the first factorial plan are similar to those obtained by Young *et al.* using non-metric multidimensional scaling (NMDS). But our algorithm of clustering reveals two classes in the first case and three classes in the second one, whereas Young *et al.* alway distinguishes only two classes. Concerning this second control case, we owe our results to our partitioning algorithm that takes into account the difference of variance-explained between the two dimensions of the diagram. The first factor (which is represented by a dorso-ventral axis) explains 51% of the variance, although the second factor (orthogonal to the first) only explains 13% of the variance. So, in the partitioning process, the first factor is much more important than the second one.

#### *4.3.2 About the Artificial Data Given by the Interpolation*

Even if we have already tested the quality of the algorithm (cf. section 2.2.3), we have also verified that the 'relay'' areas are not those which have the most artificial data given by the interpolation process. We have sorted the 30 visual areas in decreasing order of their unknown entries in the connections' matrix (cf. Fig. 9). The seven 'relay areas' – V4t, FEF, VOT, DP, 7a, FST and V4 – respectively come in 1st, 2nd, 3rd, 6th, 22nd, 27th and 29th. There are, among them, at the same time, areas with many unknowns and areas with few unknowns. More generally, we have searched for a relationship between the absolute values of the coordinates of the areas on the first factorial axis (which separates the second class from the two others) and the number of artificial data. There is no correlation between these two data series ($r^2 = 0.04$; $P = 0.31$).

### *4.4 Functional Interpretation of our Results*

We have to be very careful of excessive functional interpretations from a topological diagram, such as the one of Figure 6. As we have mentioned in the introduction, the visual areas are differentiated by anatomical or physiological criteria and then one is easily tempted to make the strong hypothesis of a functional homogeneity of each cortical area. But since we do not really know how true this hypothesis is, we remain general in our following interpretations. All of them take into account the percentages of Table 2, which may be understood as an index of reliability of the computed pairs.

The dorsal and the ventral classes revealed by the present analysis correspond to a large extent with the areas of the dorsal and ventral streams proposed by several authors (Ungerleider and Mishkin, 1982; Ungerleider and Desimone, 1986; Baizer *et al.*, 1991; Van Essen *et al.*, 1992; Young, 1992). In such a case, the 'relay' areas would be inter-stream areas allowing communication between the two streams. This interpretation is consistent with previous neurophysiological studies that conclude that FEF (Schall *et al.*, 1995), V4 and the anterior STS (Baizer *et al.*, 1991) are important in the communication between the two streams.

More precisely, the position of the three clusters of the 'relay' areas (Fig. 6) and the analysis of their projections suggest that both areas VOT and V4 are restrictive gateways between the dorsal class and infero-temporal areas; that area 7a is an interface between the upper part of each dorsal and ventral class; and that the area FEF is an important node of the visual system.

Although area 7a has properties closely allied to LIP, VIP or MST (Andersen and Gnadt, 1989; Colby *et al.*, 1993), its reciprocal connections with the upper part of the ventral class distinguish it. This particular position of area 7a, revealed in Figure 6, was already emphasized by several studies (Neal *et al.*,

1988; Andersen *et al.*, 1990). In the vision of Ungerleider and Mishkin (1982) of two hierarchical pathways of the 'what' and the 'where', this takes on great theoretical importance since area 7a links the upper parts of both streams.

The predictions of our model give to the frontal eye field reciprocal connections with every other area except V1, and nearly half of the artificial data has a percentage superior or equal to 90% in Table 2. Recent experiments showing projections from FEF to posterior cortical areas (Stanton *et al.*, 1995), between FEF and both areas V4t and PITd (Schall *et al.*, 1995), between FEF and AITv (Webster, 1994) and from V2 to FEF (Gattass, 1997) support some predictions of our model about the values of unknown projections to and from FEF. Such a central position of FEF would signify that this area plays a pivotal role in many different aspects of cortical processing.

Whereas most of connections are reciprocal (90%), nearly half the projections between the dorsal and the ventral classes are not reciprocal. They are all from the upper part of the dorsal class (intraparietal and medial superior temporal cortex) to the upper part of the ventral class (areas named STPa, TF, TH and 46), especially area 46. In addition to that, area 46 has reciprocal connections with every area of the ventral class. This suggests that it intervenes as a dispatcher in the ventral class for some aspects of visual processing which begin in the dorsal class.

Our predictions suggest the existence of projections from PO to the occipital cortex. It gives area PO similar connections to area V3A. Both areas are reciprocally connected to every area of the dorsal class and have no connection with the ventral class.

Area TF is the only area of the ventral class reciprocally connected with all the 'relay'' areas and all the areas of the ventral class. Therefore, we may consider this area either as a dispatcher on the way to the temporal areas, or, in the other direction, it could be a node which integrates multiple results of visual processing in the temporal areas before sending the information to the 'relay' areas.

Finally, the maximum value of the direct distance $e(u,v)$ on the graph $G_1$ is 3 and is attained between V1 and each of the areas STPp, STPa and AITd. There are neither direct nor indirect connections from V1 to these areas. Hence, these three areas are the farthest areas from that considered as being the main entrance of the visual information into the cortex. It reinforces the hypothesis that these areas are probably at a high level in a hierarchical visual processing (Young, 1992; Imbert and de Schonen, 1994; Hilgetag *et al.*, 1996). Even if we believe that areas STP perform an integrative role, we must not be embarrassed to put them in the ventral class. If we increase the number of classes of the partition to 6, areas STPa and STPp cut them off in a separate class. On the other hand, as these areas have no connections with the dorsal class except with areas MST, in our study it prevents them from belonging to any of the dorsal or 'relay' classes. In any cases, this position of areas STP does not preclude a highly integrative role.

## Conclusion

We have presented a new method for studying the topology of an oriented network that is not entirely known. It is based on an algorithm of topological interpolation in conjunction with other algorithms responding to vertex partitioning problems. Applied to the macaque visual system, this method supports the existence of two distinct classes of areas, one in the parietal part of the cortex and the other in the temporal part, which are connected to each other via 'relay' areas, especially involving the frontal eye field. From a general point of view, these results support recent work concluding that a functional clustering of the cortex into two segregated hierarchical streams is surely oversimplified (Schiller, 1993; Bullier *et al.*, 1995; Gegenfurtner *et al.*, 1996; Rockland *et al.*, 1996). Moreover, the very high density of internal connections within both dorsal and ventral classes makes it unlikely that the topological approach of the network alone will provide much further insight into visual processing within these two main classes.

## Notes

We thank Simon Thorpe and Hubert de Fraysseix for their comments on the manuscript. This work was partially supported by a grant from the Conseil Régional Midi-Pyrénées and by ESPRIT LTR Project no. 20244-ALCOM-IT. B.J. was supported by a grant from the MENESRIP.

Address correspondence to Bertrand Jouve, Centre de Recherche Cerveau et Cognition – UMR 5549, Faculté de Médecine de Rangueil, 133 route de Narbonne, Toulouse Cedex, France. Email: jouve@cerco.ups-tlse.fr.

## References

Andersen RA, Gnadt JW (1989) Posterior parietal cortex. In: The neurobiology of saccadic eye movements (Wurtz R, Goldberg M, eds), pp. 315–335. Amsterdam: Elsevier Science.

Andersen RA, Asanuma C, Essick G, Siegel RM (1990) Corticocortical connections of anatomically and physiologically defined subdivisions within the inferior parietal lobule. J Comp Neurol 296:65–113.

Baizer JS, Ungerleider LG, Desimone R (1991) Organisation of visual inputs to the inferior temporal and posterior parietal cortex in macaques. J Neurosci 11:168–190.

Barbas H (1988) Anatomic organization of basoventral and mediodorsal visual recipient prefrontal regions in the rhesus monkey. J Comp Neurol 276:313–342.

Bastin C, Benzecri JP, Bourgarit C, Cazes P (1980) Pratique de l'analyse des données. Tome 2. Paris: Dunod.

Benzecri JP, Benzecri F (1984) Pratique de l'analyse des données. Tome 1. Paris: Dunod.

Berge C (1983) Graphes. Paris: Bordas.

Boussaoud D, Ungerleider LG, Desimone R (1990) Pathways for motion analysis: cortical connections of the medial superior temporal and fundus of the superior temporal visual areas in the macaque. J Comp Neurol 296:462–495.

Bullier J, Nowak LG (1995) Parallel versus serial processing: new vistas on the distributed organization of the visual system. Curr Opin Neurobiol 5:497–503.

Colby CL, Gattass R, Olson CR, Gross CG (1988) Topographical organization of cortical afferents to extrastriate visual area PO in macaque: a dual tracer study. J Comp Neurol 269:392–413.

Colby CL, Duhamel JR, Goldberg ME (1993) Ventral intraparietal area of the macaque: anatomic location and visual response properties. J Neurophysiol 69:902–914.

Dice LR (1945) Measures of the amount of ecologic association between species. Ecology 26:297–302.

Distler C (1993) Cortical connections of inferior temporal area TEO in macaque monkeys. J Comp Neurol 334:125–150.

Felleman DJ, Van Essen DC (1991) Distributed hierarchical processing in the primate cerebral cortex. Cereb Cortex 1:1–47.

Fichet B, Le Calve G (1984) Structure géométrique des principaux indices de dissimilarité sur signes de présence–absence. Statist Anal Données 3:11–44.

de Fraysseix H, Kuntz P (1992) Pagination of large-scale networks. Algor Rev 2:105–112.

de Fraysseix H, Kuntz P, Rosenstiehl P (1993) NETCUT: a software for large graph partitioning. ALCOM Report. Centre d'Analyse et de Mathématiques Sociales (EHESS-PARIS), Laboratoire d'Intelligence Artificielle et Systèmes Cognitifs (TELECOM Bretagne).

Gattass R *et al.* (1997). Cortical projections of area V2 in the macaque. Cereb Cortex 7:110–129.

Gegenfurtner KR, Hawken MJ (1996) Interaction of motion and color in the visual pathways.Trends Neurosci 19:394–401.

Gower JC (1986) Euclidean distance matrices. In: Multidimensional data analysis (De Leeuw *et al.*, eds), pp. 12–22. Leiden: DWSO.

Gower JC, Legendre P (1986) Metric and Euclidean properties of dissimilarity coefficients. J Classif 3:5–48.
Harary F (1971) Graph theory. Reading, MA: Addison-Wesley.
Hebb DO (1949) The organization of behavior. New York: Wiley.
Hilgetag CC, O'Neill MA, Young MP (1996) Indeterminate organization of the visual system. Science 271:776–777.
Hof PR, Morrison JH (1995) Neurofilament protein defines regional patterns of cortical organization in the macaque monkey visual system: a quantitative immunohistochemical analysis. J Comp Neurol 352:161–186.
Imbert M, de Schonen S (1994) Vision. In: Traité de Psychologie Expérimentale (Requin and Richelle, eds), pp. 345–432. Paris: Presses Universitaires de France.
Kuntz P (1992) Representation euclidienne d'un graphe abstrait en vue de sa segmentation. Ph.D. thesis, Ecole des Hautes Etudes en Sciences Sociales, Paris.
Madison DV, Malenka R, Nicoll RA (1991) Mechanisms underlying long-term potentiation of synaptic transmission. Annu Rev Neurosci 14:379–397.
Neal JW, Pearson RCA, Powell TPS (1988) The organization of the cortico-cortical connections between the walls of the lower part of the superior temporal sulcus and the inferior parietal lobule in the monkey. Brain Res 438:351–356.
Rockland KS, Drash GW (1996) Collateralized divergent feedback connections that target multiple cortical areas. J Comp Neurol 373:529–548.
Schall JD, Morel A, King DJ, Bullier J (1995) Topography of visual cortex connections with frontal eye field in macaque: convergence and segregation of processing streams. J Neurosci 15:4464–4487.
Schiller PH (1993). The effects of V4 and middle temporal (MT) area lesions on visual performance in the rhesus monkey. Vis Neurosci 10:717–746.
Stanton GB, Bruce CJ, Goldberg ME (1995) Topography of projections to posterior cortical areas from the macaque frontal eye fields. J Comp Neurol 353:291–305.
Tootell RBH, Taylor JB (1995) Anatomical evidence for MT and additional cortical visual areas in humans. Cereb Cortex 1:39-55.
Torgerson WS (1958) Theory and methods of scaling. New York: Wiley.
Ungerleider LG, Desimone R (1986) Cortical connections of visual area MT in the macaque. J Comp Neurol 248:190–222.
Ungerleider LG, Mishkin M (1982) Two cortical visual systems. In: Analysis of visual behavior (Ingle DG, Goodale MA, Mansfield RJQ, eds), pp. 549–586. Cambridge, MA: MIT Press.
Van Essen DC, Anderson CH, Felleman DJ (1992) Information processing in the primate visual system: an integrated systems perspective. Science 255:419–423.
Webster MJ *et al.* (1994). Connections of inferior temporal areas TEO and TE with parietal and frontal cortex in macaque monkeys. Cereb Cortex 5:470-483.
Young MP (1992) Objective analysis of the topological organization of the primate cortical visual system. Nature 358:152–155.
Young MP, Scannel JW, O'Neill MA, Hilgetag CC, Burns G, Blakemore C (1995) Non-metric multidimensional scaling in the analysis of neuroanatomical connection data and the organization of the primate cortical visual system. Phil Trans R Soc Lond B 348:281–308.

## Appendix 1

### *Notations and Definitions in Graph Theory*

Given a set $V$, we denote by $W$ the set $V \times V - \{(i,i);\ i \in V\}$. We mean by *graph* a quadruplet $G = \{V,E,N,U\}$ where $V$ is a finite non-empty set of $n$ objects, called vertices (or areas), and $E$, $N$ and $U$ are three subsets of $W$ such that $\{E,N,U\}$ is a partition of $W$. By a pair $(i,j)$, we mean in the following a ordered pair of vertices with $i \neq j$. The pairs of $E$ are called *arcs* or *connections* and are $m$ in number. If both arcs $(i,j)$ and $(j,i)$ belong to $E$, they constitute a reciprocal connection. The elements of $N$ are called *non-arcs* or *non-connections*. The elements of $U$ are called 'unknown pairs'. We say that a pair $(i,j)$ is a *known pair* if it is a connection or a non-connection. If $U = \emptyset$ (i.e. $\{E,N\}$ is a partition of $W$), our definition of a graph $G$ matches that of Harary (1971) and Berge (1983). In such a case, we may just define the graph thanks to the two sets $V$ and $E$ , and we note $G = \{V,E\}$.

If the arc $e = (i,j)$ belongs to $E$, the vertex $i$ is a *predecessor* of the vertex $j$ in $G$, and the vertex $j$ is a *successor* of the vertex $i$ in $G$. By convention, a vertex $i$ is a predecessor and a successor of itself. The arc $E$ is said to be *incident from* the vertex $i$ and *incident to* the vertex $j$. The vertices $i$ and $j$ are respectively the *initial* and *final extremity* of the arc $E$.

**Definition 7** *Given a graph $G = \{V,E,N,U\}$, we define $\Gamma_G^+(i)$ as the set of the successors of the vertex $i$ in $G$:*

$$\Gamma_G^+(i) = \{j \in V, (i,j) \in E\} \cup \{i\}$$

In the same way, we define $\Gamma_G^-(i)$ as the set of the predecessors of the vertex $i$ in $G$:

$$\Gamma_G^-(i) = \{j \in V, (j,i) \in E\} \cup \{i\}$$

The *adjacency matrix* $A(G)$ of a graph $G$ is an $n \times n$ matrix $(a_{ij})$ with $a_{ij} = 1$ if $(i,j)$ is an arc of $G$ or $i = j$, and $a_{ij} = 0$ if $(i,j)$ is a non-arc or an unknown arc of $G$. This matrix is not generally a symmetrical matrix. Note that this definition of $A(G)$ confuses non-connections and unknown pairs.

A *supergraph* of a graph $G$ is a graph with the same vertices as $G$ and containing all the connections and non-connections of $G$.

A subgraph of a graph $G$ is a graph $(V',E',N',U')$ with $V' \subset V$ and $E'$, $N'$ and $U'$ are the respective intersections of $E$, $N$ and $U$ with $V' \times V'$.

### *Density of a Graph*

**Definition 8** *Given a graph $G$ with $n$ vertices and $m$ arcs, we define its density as the ratio $m/n(n-1)$.*

The density is a number between 0 and 1, equal to the number of arcs of $G$ divided by the total number of possible arcs of $G$.

## Appendix 2

Given $I_p = (I_1,I_2,\ldots,I_p)$ an ordered $p$-list of binary integers, let us denote $|I_p - J_p|$ the distance between the two lists $I_p$ and $J_p$ defined by:

$$|I_p - J_p| = \sum_{k=1}^{p} |i_k - j_k|$$

We denote by $\binom{p}{k}$ the integer $p!/k!(p-k)!$.

**Proposition 1** *The mean distance between two binary ordered $p$-lists is $p/2$.*

**Proof** Given an integer $k$ between 1 and $p$ and a binary ordered $p$-list $I_p$, there are $\binom{p}{k}$ ordered $p$-lists whose distance with $I_p$ is $k$. Thus, the mean distance between two binary ordered p-lists is:

$$\frac{1}{2^p} \sum_{k=1}^{p} k \binom{p}{k}$$

The use of the two combinatorial formulas

$$\binom{p}{k} = \frac{p}{k} \cdot \binom{p-1}{k-1} \quad \text{and} \quad 2^p = \sum_{k=1}^{p} \binom{p}{k}$$

immediately gives:

$$\frac{1}{2^p} \sum_{k=1}^{p} k \binom{p}{k} = \frac{p}{2}$$

and the result. ■

## Appendix 3: A Distance on the Vertices of an Oriented Graph

**Definition 9** *Given a graph G, we denote* $\delta^+$ *and* $\delta^-$ *the mappings of V × V in [0;1] such that:*

$$\left(\delta^+\right)^2(i,j)=\frac{\left|\Gamma_G^+(i)\triangle\Gamma_G^+(j)\right|}{\left|\Gamma_G^+(i)\right|+\left|\Gamma_G^+(j)\right|}=\frac{\sum_{k=1}^{n}\left|a_{ik}-a_{jk}\right|}{\sum_{k=1}^{n}\left(a_{ik}+a_{jk}\right)}$$

$$\left(\delta^-\right)^2(i,j)=\frac{\left|\Gamma_G^-(i)\triangle\Gamma_G^i(j)\right|}{\left|\Gamma_G^-(i)\right|+\left|\Gamma_G^-(j)\right|}=\frac{\sum_{k=1}^{n}\left|a_{ki}-a_{kj}\right|}{\sum_{k=1}^{n}\left(a_{ki}+a_{kj}\right)}$$

*where A* $\triangle$ *B symbolizes the symmetric difference between the two sets A and B, i.e. the set of elements that belong exactly to one of the two sets A, B.*

$(\delta^+)^2$ is called the Czekanowski–Dice coefficient for the matrix $A(G)$ (Dice, 1945). Because $A(G)$ is a binary matrix, $\delta^+$ is a distance (Gower and Legendre, 1986). As $(\delta^-)^2$ is the Czekanowski–Dice coefficient for the transpose matrix ${}^{T}A(G)$, $\delta^-$ is also a distance. Notice that $\delta^+(i,j)$ [resp. $\delta^-(i,j)$] is equal to 0 if and only if the vertices $i$ and $j$ have the same successors (resp. predecessors).

A distance $d$ on a set $V$ is Euclidean if the metric space $V$ can be isometrically embedded in $\mathbb{R}^k$ with respect to $d$.

Let $\Re$ be the equivalence relation $i\Re j \Leftrightarrow \delta(i,j) = 0$ and $d^+$ and $d^-$ the functions respectively induced by $\delta^+$ and $\delta^-$ on $V/\Re \times V/\Re$: $d^+$ and $d^-$ are Euclidean distances on $V/\Re \times V/\Re$ (Fichet and Le Calve, 1984; Gower, 1986).

**Definition 10** *Given a graph G, we denote by d the mapping of* $V/\Re \times V/\Re$ *in [0;1] such that:*

$$d^2=\frac{1}{2}\left(\left(d^+\right)^2+\left(d^-\right)^2\right)$$

**Proposition 2** *The mapping d is a Euclidean distance on* $V/\Re \times V/\Re$.

### *Embedding V in the Euclidean space* $\mathbb{R}^k$

Let us consider a Euclidean distance $d$ on a vertex set $V$ of an abstract graph $G$; a $d$-embedding $I_d(G)$ of $G$ in the space $\mathbb{R}^k$ is a mapping of $V$ in $\mathbb{R}^k$ that is isometric with respect to $d$. Let $(\mathbf{i}_p)_{1 \le p \le k}$ and $(\mathbf{j}_p)_{1 \le p \le k}$ be the coordinates of vertices $i$ and $j$ in $\mathrm{R}^k$, the Euclidean distance

$$\left(\sum_{p=1}^{k}\left(\mathbf{i}_p-\mathbf{j}_p\right)^2\right)^{\frac{1}{2}}$$

is equal to the distance $d(i,j)$ between the vertices $i$ and $j$. If $n = |V|$, $V$ has a $d$-embedding in $\mathbb{R}^{n-1}$. The geometric representation $I_d(G)$ is easier to analyze if $d$ is Euclidean because it has no distortion.

### *Factorial Analysis of* $I_d(G)$

*Factorial Axes*

We consider new coordinate axes, $(\Delta_p)_{p \ge 1}$, in the space $\mathbb{R}^k$, generated by vectors $(F_p)_{p \ge 1}$, centered on the center of gravity of $I_d$(G), and around which the vertices are organized. These axes are called factorial axes. If $(\mathbf{i}_1, \mathbf{i}_2, \ldots, \mathbf{i}_k)$ are the coordinates of a vertex $i$ in this new system of reference, we define the inertia $i_S$(G) of the graph $G$ in the subspace $S$ generated by $(F_{p1}, F_{p2}, \ldots, F_{pk})$:

$$i_S(G)=\sum_{j=1}^{k} i_{\Delta_{p_j}}(G)$$

where

$$i_{\Delta_{p_j}}(G)=\frac{1}{n}\cdot\sum_{i=1}^{n}\left(\mathbf{i}_{p_j}\right)^2$$

$\Delta_1$ is the axis onto which the inertia of the projection of $I_d$(G) is maximum, $\Delta_2$ is the axis orthogonal to $\Delta_1$ such that the inertia of the projection of $I_d$(G) onto the subspace $(\Delta_1,\Delta_2)$ is maximum, and so on, $\Delta_p$ is the axis orthogonal to the subspace $(\Delta_1, \ldots, \Delta_{p-1})$ such that the inertia of the projection of $I_d$(G) onto the subspace $(\Delta_1, \ldots, \Delta_p)$ is maximum. Then, each axis $\Delta_p$ is associated with a direction of maximal stretch of $I_d$(G). Each coordinate, in this new coordinate system, is called a factor. The factors are in decreasing order from the first to the $p$th.

Let $D = (d_{ij})_{1 \le i,j \le n}$ be the $n \times n$ matrix of the distances $d$ on the graph $G$, and $\Omega = (\omega_{ij})_{1 \le i,j \le n}$ the matrix defined by:

$$\omega_{ij}=\frac{1}{2}\left(d^2(i,.)+d^2(.,j)-d^2(i,j)-d^2(.,.)\right)$$

where

$$d^2(i,.)=\frac{1}{n}\sum_{j=1}^{n}d^2(i,j) \quad \text{and} \quad d^2(.,.)=\frac{1}{n}\sum_{i=1}^{n}d^2(i,.)$$

If $d$ is Euclidean, the bilinear symmetric form associated with the matrix $\Omega$ is positive semi-definite (Torgerson, 1958). In such a case, if $\lambda_p$ are the eigenvalues of $\Omega$, they are positive, and supposing they are arranged in descending order, the corresponding eigenvectors are the $F_p$s' and then guide the axes $\Delta_p$.

*Contributions*

If $k$ is the dimension of the embedding space, for all $p \in [1;k]$, the eigenvalue $\lambda_p$ is equal to the inertia $i_{\Delta_p}(G)$ of $G$ along $\Delta_p$ (Benzecri, 1984), and

$$\tau_p=\frac{\lambda_p}{\sum_{j=1}^{k}\lambda_j}$$

gives the importance of the factor $p$ in the representation of $G$. We denote by $COR_p(i)$ the relative contribution of the factor $p$ to the distance between the vertex $i$ and the center of gravity of $I_d$(G):

$$COR_p(i)=\frac{\left(\mathbf{i}_p\right)^2}{\sum_{l=1}^{k}\left(\mathbf{i}_l\right)^2}$$

$COR_p(i) + COR_q(i)$ gives the quality of the representation of the vertex $i$ in the factorial plan $(p,q)$. We denote by $CTR_p(i)$ the relative contribution of the vertex $i$ to the inertia $i_{\Delta_p}(G)$ of $G$ along the $p$th factorial axis:

$$CTR_p(i)=\frac{\left(\mathbf{i}_p\right)^2}{\sum_{j=1}^{n}\left(\mathbf{j}_p\right)^2}$$

Given an integer $p$, the analysis of the distribution of the $CTR_p(i)$ can be used to decide if the inertia of the axis $p$ results only from some vertices, which have a large $CTR_p$, or results from all the vertices of the cloud.